J Appl Physiol 116: 790–796, 2014.
First published January 16, 2014; doi:10.1152/japplphysiol.01156.2013.

Microbubbles are detected prior to larger bubbles following decompression

J. G. Swan,[1] J. C. Wilbur,[2] K. L. Moodie,[1] S. A. Kane,[1] D. A. Knaus,[2] S. D. Phillips,[2] T. L. Beach,[2] A. M. Fellows,[1] P. J. Magari,[2] and J. C. Buckey[1]

[1]*Geisel School of Medicine, Dartmouth University, Hanover, New Hampshire;* [2]*Creare, Hanover, New Hampshire*

Submitted 16 October 2013; accepted in final form 14 January 2014

Swan JG, Wilbur JC, Moodie KL, Kane SA, Knaus DA, Phillips SD, Beach TL, Fellows AM, Magari PJ, Buckey JC. Microbubbles are detected prior to larger bubbles following decompression. *J Appl Physiol* 116: 790–796, 2014. First published January 16, 2014; doi:10.1152/japplphysiol.01156.2013.—Using dual-frequency ultrasound (DFU), microbubbles (<10 μm diameter) have been detected in tissue following decompression. It is not known if these microbubbles are the precursors for B-mode ultrasound-detectable venous gas emboli (bmdVGE). The purpose of this study was to determine if microbubbles could be detected intravascularly postdecompression and to investigate the temporal relationship between microbubbles and larger bmdVGE. Anesthetized swine (n = 15) were exposed to 4.0–4.5 ATA for 2 h, followed by decompression to 0.98 ATA. Microbubble presence and VGE grade were measured using DFU and B-mode ultrasound, respectively, before and for 1 h postdecompression, approximately every 4–5 min. Microbubbles appeared in the bloodstream postdecompression, both in the presence and absence of bmdVGE. In swine without bmdVGE, microbubbles remained elevated for the entire 60-min postdecompression period. In swine with bmdVGE, microbubble signals were detected initially but then returned to baseline. Microbubbles were not detected with the sham dive. Mean bmdVGE grade increased over the length of the postdecompression data collection period. Comparison of the two response curves revealed significant differences at 5 and 10 min postdecompression, indicating that microbubbles preceded bmdVGE. These findings indicate that decompression-induced microbubbles can *1*) be detected intravascularly at multiple sites, *2*) appear in the presence and absence of bmdVGE, and *3*) occur before bmdVGE. This supports the hypothesis that microbubbles precede larger VGE bubbles. Microbubble presence may be an early marker of decompression stress. Since DFU is a low-power ultrasonic method, it may be useful for operational diving applications.

ultrasound; decompression sickness; dual-frequency ultrasound; venous gas emboli

FOLLOWING DECOMPRESSION, VENOUS gas emboli (VGE) may appear in the bloodstream (10). These emboli are readily detected by B-mode ultrasound in the chambers of the right heart. With moderate decompression stress, VGE often appear as occasional bubbles initially (VGE Grade 1) and then can progress over time to large amounts of bubbles (1 bubble every cm^2, VGE Grade 4) or even complete whiteout (VGE Grade 5) as described by Brubakk and Efetal (6). VGE grade correlates positively with the rate of ascent. Although VGE grade does not reliably predict decompression sickness (DCS) symptoms, it is used as a marker of decompression stress. Eftedal et al. proposed that bubble detection using B-mode ultrasound imaging could be used as a tool to assess the safety of decompression procedures (11). If, for example, a particular prebreathing strategy was effective at preventing the appearance of VGE, then this procedure could also be effective at preventing decompression sickness.

Larger VGE bubbles likely begin as smaller microbubbles, and so smaller microbubbles should appear in the vascular system prior to larger VGE bubbles (3, 17, 22, 24). In theory, if microbubbles could be detected at the microbubble stage, this might provide earlier detection of decompression stress than standard VGE detection provides. Such a marker could potentially be used to prevent decompression sickness, by giving the diver advance warning of bubble formation and allowing for countermeasures to be employed (e.g., by using longer or deeper decompression stops).

Until recently, the technology to detect microbubbles at physiological concentrations has not been available. In previous work, we have shown that dual-frequency ultrasound (DFU), which generates ultrasound returns from bubbles but not other linear reflectors, can detect microbubbles. DFU can be used to size microbubbles in vitro (4), detect small microbubbles in tissue produced by exercise (23), and detect bubbles in tissue after decompression (21).

The goal of the present study was to determine if DFU could detect decompression-induced microbubbles in the vascular system and whether these bubbles would precede the appearance of B-mode ultrasound-detectable VGE (bmdVGE). We established the sensitivity of DFU for detecting ultrasonic contrast agent (Definity, Bristol-Myers Squibb, N. Billerica, MA) in an in vitro study. Also using ultrasonic contrast, we confirmed that the DFU could detect injected microbubbles at vascular sites. We then monitored decompression-induced bubbles at three vascular and one extravascular tissue sites in 15 swine exposed to decompression and one sham dive. We hypothesized that DFU could detect microbubbles at both vascular and tissue sites and that this detection would precede bmdVGE.

METHODS

The Dartmouth Institutional Animal Care and Use Committee approved the animal-related research protocols.

DFU signal collection. The dual-frequency technique used to detect microbubbles has been described elsewhere, so it will be described only briefly here (5, 7). Two continuous wave frequencies of ultrasound (2.25 and 5 MHz) interrogate the area to be measured, and the return signal is simultaneously recorded. The presence of microbubbles is determined by the strength of the returning signal at the difference of the two interrogating frequencies (e.g., 2.75 MHz). An increase in the difference signal from baseline was used as a measure of microbubble presence. To determine the difference signal, we performed a fast-Fourier transform (FFT), a mathematical algorithm expressing data in the frequency domain, of the time-dependent electrical signal returned via the receive transducer. We recorded the amplitude of the frequency spectrum at the difference frequency (the "difference signal") as well as the average noise of the spectrum near the difference frequency (calculated as the median signal level within a few 10,000 Hz on either side of the difference frequency). The

Address for reprint requests and other correspondence: J. G. Swan, Geisel School of Medicine at Dartmouth, One Medical Center Dr., Lebanon, NH 03756 (e-mail: Jacob.g.swan@dartmouth.edu).

amplitude of the difference signal is reported in the results section both in units of decibels relative to the background noise amplitude (signal-to-noise ratio, dB SNR) and as decibels relative to the mean signal amplitude collected during the baseline measurements (signal-to-baseline ratio, referred to here as dB SBR). The dB SNR metric is an absolute measurement as the noise floor of the system remained effectively constant for all experiments, while the SBR metric is a relative measure designed to capture changes between the baseline and postdive measurements. Generally, the SBR is 1–3 dB lower than the SNR.

DFU sensitivity study. To assess the sensitivity limit of DFU, we compared the returned difference signal from decreasing concentrations of microbubbles to the return from a control solution with no microbubbles. Ultrasound contrast agent (Definity; diameter = 1–3 μm) was activated according to the manufacturer's specifications and diluted to specified concentrations in degassed saline. The control solution was saline that contained no ultrasound contrast agent and had been degassed to eliminate any bubbles. Approximately 70 mL of the test concentrations were placed in a plastic test vial. A holder was built to hold both the test vial and the DFU transducers in place to minimize any variation due to positioning. The holder, along with transducers and test vial, were then placed into an aquarium where the tests were conducted. The aquarium was filled with mineral oil and lined with acoustically suppressing tile (Apflex F28, Precision Acoustics, Dorchester, UK) to minimize standing waves. The returned difference signal was measured in triplicate for each concentration and in rotational order. Comparisons were made between the control solutions and each microbubble concentration.

For comparison, we determined the sensitivity for the B-mode ultrasound device (Ultrasonix, Sonix RP) we used in our swine studies using the same procedure. The ultrasound transducer was placed into the aquarium with the test vials. Each vial was measured in triplicate at 6.6 MHz and 10 MHz settings; all ultrasound settings were kept identical for each measure within each transducer setting. Grayscale pictures were taken and analyzed for pixel intensity inside the test vial (Image J). Comparisons were made between the control solutions and each microbubble concentration.

Detection of microbubbles at vascular sites. To verify that the DFU unit could detect microbubbles in the vasculature, ultrasound contrast agent (Definity; bolus injection = 10 μL/kg as per manufacturer's instructions) was injected into ear vein IV line and the vascular return difference signal was measured. All experiments were performed on 12-wk-old, ~20 kg female swine (Parson's Farm, Westhampton, MA). Swine were initially anesthetized using 20 mg/kg ketamine and 0.05 mg/kg xylazine, and then anesthesia was maintained with bolus injections of pentobarbital. The returned difference signal was measured over the following anatomical sites: the femoral, brachial, and carotid vascular bundles. These sites were located prior to injection using Doppler ultrasound and marked. DFU data were collected at each site for ~4 min prior to injection and ~10 min postinjection.

Detection of decompression-induced microbubbles. Microbubble appearance was monitored following decompression in swine. Swine were initially anesthetized using 20 mg/kg ketamine and 2.0 mg/kg xylazine and maintained with bolus injections of pentobarbital (total dose = 20 mg/kg) administered through a peripheral IV line. Since the baseline period prior to the chamber dive included breathing 100% oxygen, which could influence whether VGE were produced, the prebreathe time was standardized at 45 min for all swine. A pulse oximeter was placed on the ear for monitoring O_2 saturation and pulse.

Anesthesia was maintained inside the hyperbaric chamber by bolus injections of pentobarbital (3–10 mg/kg/h) via a chamber pass-through. At the conclusion of the hyperbaric exposure, swine were removed from the chamber, and anesthesia was maintained using isoflurane.

Dive chamber protocol. Following baseline data collection (0.98 ATA), swine were placed into the hyperbaric chamber (Reimers model 20–48). Initially, swine were compressed to 4.0 ATA at a rate of 0.6 ATA/min (n = 8). Few swine developed VGE using this protocol, so the compression pressure was increased to 4.5 ATA (n = 7). Swine were held at maximum pressure for a total of 120 min (Fig. 1). After this time period, the swine were decompressed to 0.98 ATA pressure at a rate of −0.6 ATA/min. The swine were then removed from the chamber, the pass-through catheter was disconnected, and the chamber pulse oximeter was removed. As soon as possible following the return of the swine to 0.98 ATA, postdive measurements were begun (time = 0 min). For the sham dive, the swine experienced the exact same sequence and time course of events as outlined above. The sham dive, however, did not involve compression/decompression. The sham swine was put on anesthesia and placed in the hyperbaric chamber but remained at 0.98 ATA pressure for the 120 min of dive time.

Pre and postdive data collection protocol. Data were collected before the dive and following decompression. Difference signals were collected at four anatomic sites: three vascular sites (carotid, brachial, and femoral vascular bundles) and one tissue site (lateral biceps femoris). The tissue site was used since previous research had shown that microbubbles could also be detected in tissue. Each site was located and scanned using a clinical B-mode ultrasound machine (Ultrasonix, Sonix RP) to ensure that no potential strong ultrasound reflectors (i.e., bones or joints), which could generate false positive signals, were in the measurement volume. The vascular sites were located using B-mode and verified using Doppler ultrasound. Baseline difference signals were obtained over ~5 min (300 measures). Post-decompression, difference signals were collected at each site for ~30 s (30 measures), cycling through each site multiple times in a fixed order. Each site was measured approximately once every 4–5 min. Multiple scan cycles were completed for 1 h after decompression or until skin mottling consistent with skin bends (cutis marmorata) appeared over the measurement sites. Cutis marmorata at the measurement sites was used as an end point because previous experience has shown that once this point is reached, gas in the skin hinders ultrasound transmission, making it difficult to obtain measurements.

VGE grading. VGE grade was assessed using B-mode ultrasound (Ultrasonix, Sonix RP) to image the right ventricle. VGE grade was assessed prior to entering the hyperbaric chamber and every 5 min postdecompression, beginning as soon as possible after the swine exited the chamber (time = 0 min). Video from the right ventricle obtained following the chamber dives were stored and analyzed at a later time point. Swine were given a score between 0 and 5 using the criteria outlined in Brubakk and Eftedal (6).

Statistical analysis: Sensitivity study. To determine the sensitivity threshold of DFU, the difference signal measurements from all three trials were averaged and compared with the saline-filled target control using a two-way t-test. Similarly, the B-mode ultrasound sensitivity threshold was determined by averaging the pixel intensity from all three trials and comparing each trial to the saline-filled target control using a two-way t-test.

Statistical analysis: Dive study. Swine were divided into two groups based on the level of VGE present postdecompression. Swine with VGE ≥ 3 (at least one bubble every heart cycle) at any time point

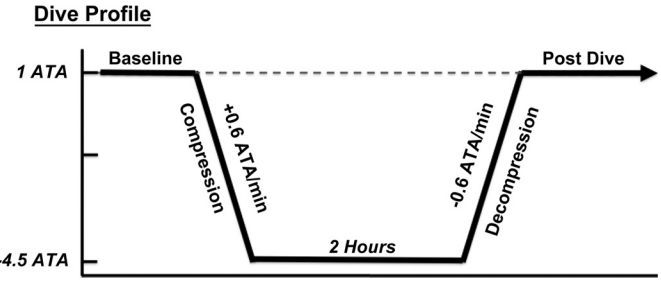

Fig. 1. Dive profile. Eight swine were compressed at 4.0 ATA; seven swine were compressed to 4.5 ATA.

were placed into the VGE High group. Swine with VGE < 3 at all time points were grouped in the VGE Low group.

Prior to statistical analysis, difference signal data (in dB SBR), both pre and postdive, were first organized into 5-min epochs for each swine. The average for each epoch was then computed across swine. To determine if microbubbles were increased over baseline, normality of data was first assessed using the Kolmorogov-Smirnov test, with $P < 0.05$ indicating a nonnormal distribution. This test showed that our difference signal data were not normally distributed so the nonparametric Friedman test was used to determine differences between baseline and any postdecompression time point within each VGE group. If the Friedman test indicated a significant difference in the data set, a post hoc comparison using the Wilcoxon signed rank test was run to determine which time epochs were significantly different. Time epochs were considered statistically different if their p value was less than p value adjusted for multiple comparisons using the Bonferroni approach ($n = 13$ comparisons; critical p value $= 0.003$).

All data are presented as average ± standard deviation, except for VGE data which are presented as medians. P values are stated when appropriate.

RESULTS

DFU sensitivity study. The sensitivity of DFU was 10 microbubbles per mL ($P < 0.01$; Fig. 2, *top*). This concentration may be an absolute physical limit on the sensitivity of any DFU-based nonlinear technique. Modeling of the effective nonlinear acoustic coefficient for difference signal generation by microbubble-containing liquids [following the technique used in (13)] shows that the added nonlinearity due to the microbubbles (relative to the host liquid) quickly becomes very small below concentrations of roughly 100 microbubbles/mL. Attempts to raise the SNR to improve sensitivity further (e.g., higher ultrasound intensity, increased averaging) always uniformly increased the measured difference signal independent of the target (e.g., saline control or microbubble solution). The sensitivity for the 6.6-MHz B-Mode imaging ultrasound in the same experimental facility was 10^4 microbubbles/mL, while the sensitivity for the 10-MHz B-mode imaging ultrasound was 10^3 microbubbles/mL (Fig. 2, bottom).

Detection of injected microbubbles in the vasculature. Injection of ultrasound contrast agent was detected in all vascular sites (Fig. 3). The time to peak signal was ~45 s using DFU, compared with the manufacturer's published time to maximum intensity using B-mode ultrasound of 1.13 min (1). Following the measured peak, the signal decayed to baseline over a period of ~7 min. This time was similar to the published decay times for Definity (1). These data verify that DFU is capable of detecting circulating microbubbles at vascular sites.

Postdecompression. A total of 15 swine were exposed to the dive profile shown in Fig. 1, plus one swine undergoing a mock dive. All swine were able to complete the full hour of data acquisition following decompression. Cutis marmorata (aka skin bends) was noted in three of the swine following decompression but was not located at the measurement sites and therefore did not interfere with data collection. Eight swine underwent compression to 4.0 ATA, of which two developed VGE >3. Seven swine underwent compression to 4.5 ATA, of which three developed VGE >3. Figure 4 (*top*) is a representative graph from one swine showing the returned difference signal at the four anatomical sites and the measured VGE.

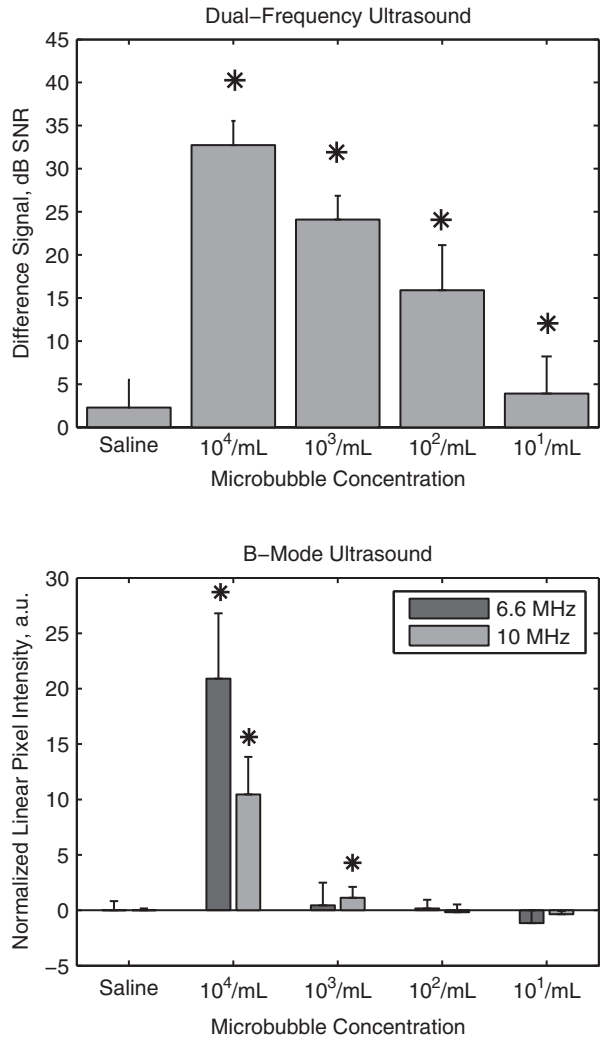

Fig. 2. Sensitivity for dual-frequency ultrasound (DFU) and B-mode ultrasound devices used in the study. (*top*) DFU was able to identify microbubbles statistically down to a concentration of 10 microbubbles/mL (*$P < 0.01$ compared with saline). (*bottom*) Using 6.6-MHz B-mode ultrasound microbubble sensitivity was 10^4 microbubbles/mL (*$P < 0.05$ compared with saline). Using 10-MHz B-mode ultrasound microbubble sensitivity was 10^3 microbubbles/mL (*$P < 0.05$ compared with saline). Error bars show +/− 1 standard deviation.

Figure 4 (*bottom*) shows only the femoral site from the same swine in the top graph.

The VGE data indicated that swine could be divided into two groups based on the amount of VGE measured postdecompression. One group, VGE High, contained swine with bmdVGE ≥ 3 at any time point ($n = 5$). The second group, VGE Low, contained swine with bmdVGE ≤ 1 at all time points ($n = 10$). Both the VGE High and VGE Low groups showed increases in microbubble signals above baseline (see Fig. 5), while the mock dive swine did not show any increase over baseline. The VGE High group (Fig. 5, *left*) showed an increase in difference signal above baseline immediately postdive at t = 0, 5, and 10 min, and then the difference signal returned to baseline. This pattern suggests an initial rise in microbubbles, followed by a decrease. The VGE Absent group (Fig. 5, *center*) also showed an immediate increase in difference signal (t = 5 and 10 min) but difference signals were also significantly above baseline at

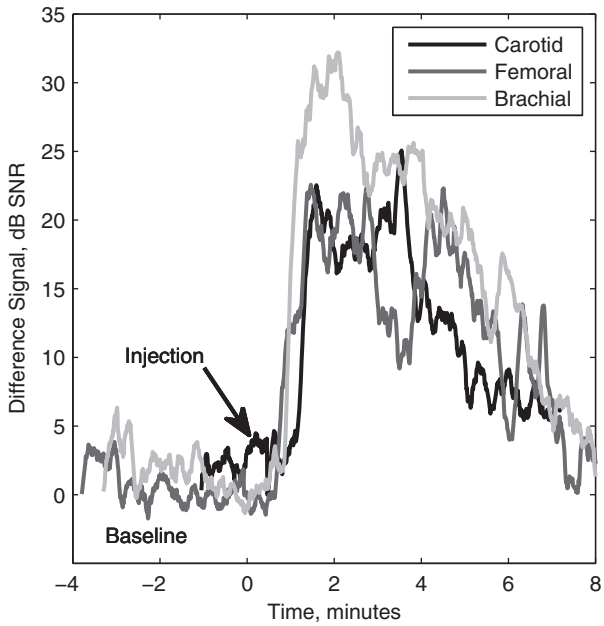

Fig. 3. Detection of ultrasound contrast agent/microbubbles at three vascular sites.

later time points (t = 30 and 45). This pattern suggests a rise in microbubbles that continued throughout the postdecompression time period. Taken together, these results suggest an inverse relationship between microbubbles and VGE grade. The VGE High group showed that as bmdVGE increased, microbubbles decreased. Conversely, in the VGE Low group, bmdVGE stayed low during the postdecompression period, while microbubbles increased and remained elevated. The data from the sham dive are plotted for comparison (Fig. 5, *right*).

DISCUSSION

The results of this study indicate that *1*) the sensitivity of DFU in vitro is on the order of 10 microbubbles/mL in water, which may represent a physical limit; *2*) DFU can be used at several vascular sites to detect microbubbles in the circulation; *3*) microbubbles are also detected at extravascular tissue sites; *4*) microbubbles appear postdecompression regardless of the VGE grade; and *5*) an inverse relationship may exist between microbubbles and bmdVGE.

DFU sensitivity study. The sensitivity of DFU, 10 microbubbles/mL, was similar to theoretical limits as predicted by the nonlinearities of microbubbles in water. In the same experimental facility, the microbubble concentration sensitivity for the B-mode ultrasound machine used in our study was found to be either 100X or 1000X less than DFU, depending whether 6.6 MHz or 10 MHz transducer frequency, respectively, was used. These results clearly show that DFU is more sensitive to microbubbles than B-mode ultrasound in vitro. The concentration of microbubbles in the bloodstream following decompression is unknown, but the microbubble concentrations likely start small and progress to higher levels. At these smaller concentrations, DFU shows a clear advantage over B-mode ultrasound in vitro. Whether the same concentration sensitivity is achieved in swine depends on several factors. The sensitivity in vivo is a function of both the target nonlinearity (i.e., microbubble concentration) and the system geometry (acoustic propagation paths and geometric distribution of the microbubbles along the paths). It is not possible to say with confidence that a measured difference signal level in one experiment (e.g., a swine) corresponds to the same microbubble concentration measured in the sensitivity study.

Nevertheless, this level of sensitivity makes this technique suitable for detecting small concentrations of bubbles. In studies using B-mode ultrasound to identify microbubbles (e.g., to detect wall motion abnormalities or vascular tumors), positive identification relies on high concentrations of microbubbles. The multiple bubbles within the ultrasound contrast agent increases backscatter of the ultrasound and increases contrast within the images. But, at lower concentrations, B-mode ultrasound is unable to differentiate small numbers of ultrasound contrast bubbles from background reflectors. Our data show that the DFU is capable of distinguishing microbubbles with specificity at very low concentrations. The absence of a clear microbubble return in the B-mode images is most likely due to insufficient microbubble concentrations relative to other linear scatter in the images.

Vascular detection of microbubbles. Our previous research has shown that DFU can detect microbubbles injected into the biceps femoris tissue sites and decompression-induced microbubbles at tissue sites (biceps femoris) in swine (5, 21). The current research investigated if DFU could be used to detect decompression-induced microbubbles within the vascular system. The data show that either the carotid, brachial, or femoral sites can be used to detect vascular bubbles with DFU.

The time course of vascular detection showed a rapid rise after bolus injection, followed by a decline. Microbubbles detected after bolus injection were detectable for ~7 min. This rate of decline matches the published half-life time (1) and is similar to what is seen in clinical use of ultrasound contrast agents (8). Injected microbubbles were detected at the three measurement sites, with each site exhibiting the same response. These vascular sites, carotid, brachial, and femoral, were chosen for two reasons. One is that these vessels were large and therefore we would be assured that the injected microbubbles would be passing through them. Two, these vessels were relatively superficial, lying anywhere from 1 to 4 cm deep, falling into the measurement volume of our machine, which is an approximate 5 mm^3 cylinder centered 2.5 cm deep. These results indicate that DFU is capable of detecting microbubbles in vascular sites.

Microbubble detection following decompression. In swine decompressed from 4.0 ATA, 2/8 had bmdVGE, while in the 4.5 ATA swine, 3/7 had bmdVGE. As in humans, there was interswine variation in the development of bmdVGE (10). Following decompression, microbubbles were detected at all the vascular sites, as well as over the tissue site (i.e., biceps femoris). No site showed a greater propensity for microbubbles over the others. These data suggest that DFU could be used at a variety of sites on the body to detect microbubbles, including tissue sites, which would be useful operationally in diving. We are most likely detecting microbubbles between 1 and 4 μm in diameter, as our ultrasound interrogation frequencies (2.25 and 5.00 MHz) are tuned for bubbles of that size (assuming they respond similarly to free air bubbles in water). The environment surrounding the bubbles (e.g., the local fluid density and pressure, location of the bubble relative to vessel walls, and the

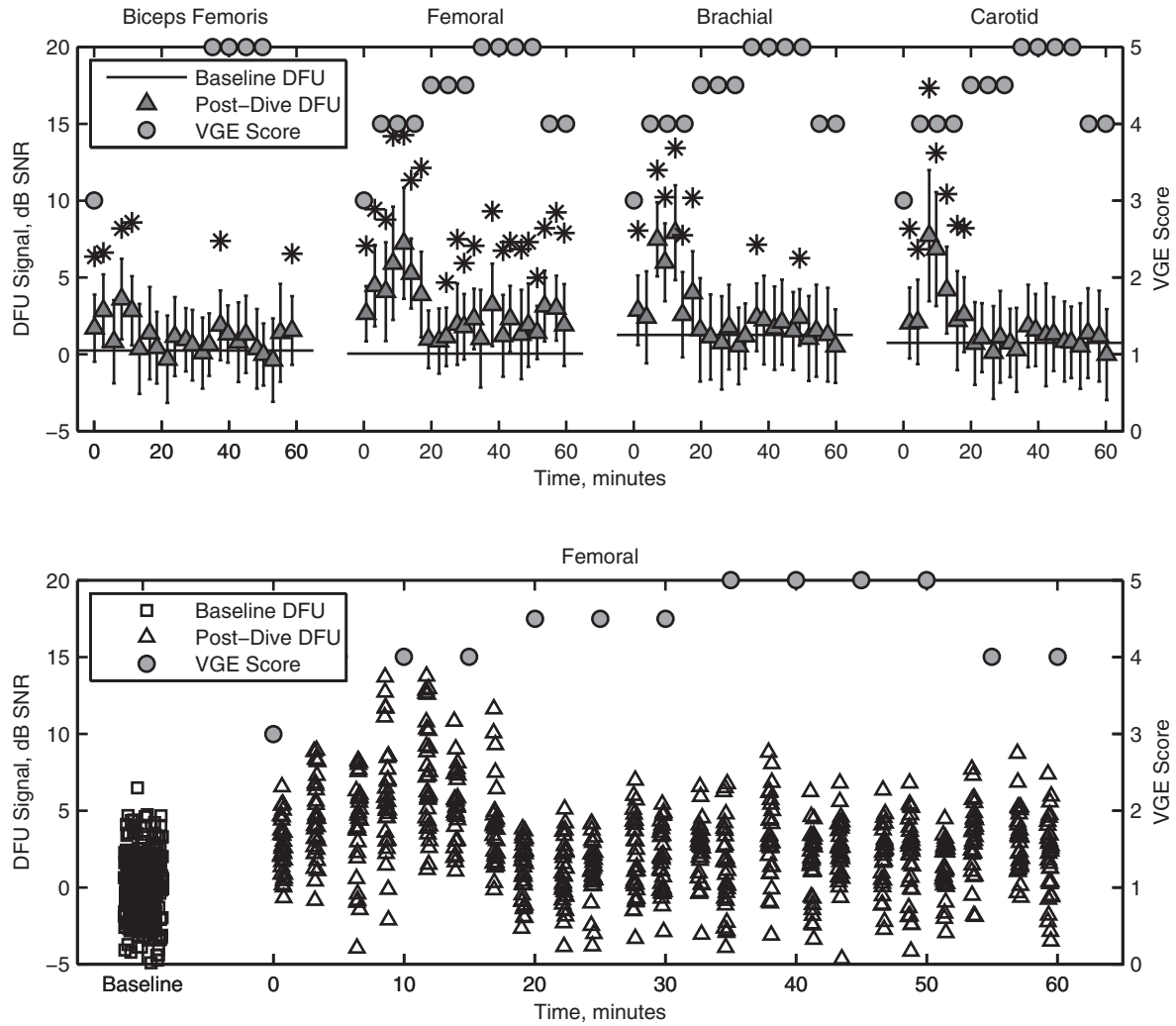

Fig. 4. (*top*) Representative data from one swine. Graphs show both the microbubble signal (avg ± SD) at four anatomic locations and the venous gas emboli (VGE) score postdecompression. *indicates microbubble signal greater than the average baseline ($P < 0.01$). (*bottom*) Graph showing the microbubble signal at baseline and postdecompression from one swine at the femoral vascular bundle. Each symbol represents an individual measurement.

presence of any bubble shell) can influence their resonant frequency, thus altering the relationship between diameter and resonant frequency. Nevertheless, it is unlikely that these factors would alter the resonant characteristics dramatically from the normative values in water, and the bubbles detected by the DFU are likely less than 10 μm. At present, there is no independent method to ascertain this in vivo.

Our results show that microbubbles were present in swine that developed VGE and also in those that did not. Microbubbles increased immediately postdecompression in both groups of swine. In the VGE High group, microbubbles decreased over time, while the VGE grade increased. The reasons for the reduction in the microbubble signal are unclear. One reason may be that smaller microbubbles are the precursors to larger VGE. Over time postdecompression, the smaller microbubbles may decrease in number as they grow to become larger bmdVGE, resulting in the increase in VGE grade. The hypothesis that microbubbles are bmdVGE prescursors has been discussed previously (3, 17, 22, 24) but the technology to prove this has been missing. The appearance of bmdVGE, and disappearance of microbubbles, may indicate that the balance of forces between bubble growth and bubble destruction (e.g., local nitrogen partial pressure, surface tension) has shifted toward bubble growth. As the bubbles grow or coalesce, they move out of the detectable range for the DFU, thereby reducing the returned DFU signal. This hypothesis is further supported by the results from the VGE Low group. This group showed increased microbubbles but little to no bmdVGE over the course of the entire postdecompression period. This suggests that there was no progression of smaller microbubbles to larger VGE. While these data do not prove that microbubbles grow or coalesce to form bmdVGE, these data support the hypothesis that bmdVGE begin as microbubbles.

A second explanation for the decrease in microbubble signal over time is that as VGE appear in the bloodstream, it is possible that they scatter the ultrasound signal and reduce the ultrasound incident on the microbubbles. The level of microbubbles may not actually change but only appear to change due to scattering of the ultrasound. An analysis of the returned frequencies (data not shown) do not show a diminution of either the pump or image frequency. Had the VGE been scattering the return signals, we would have expected a de-

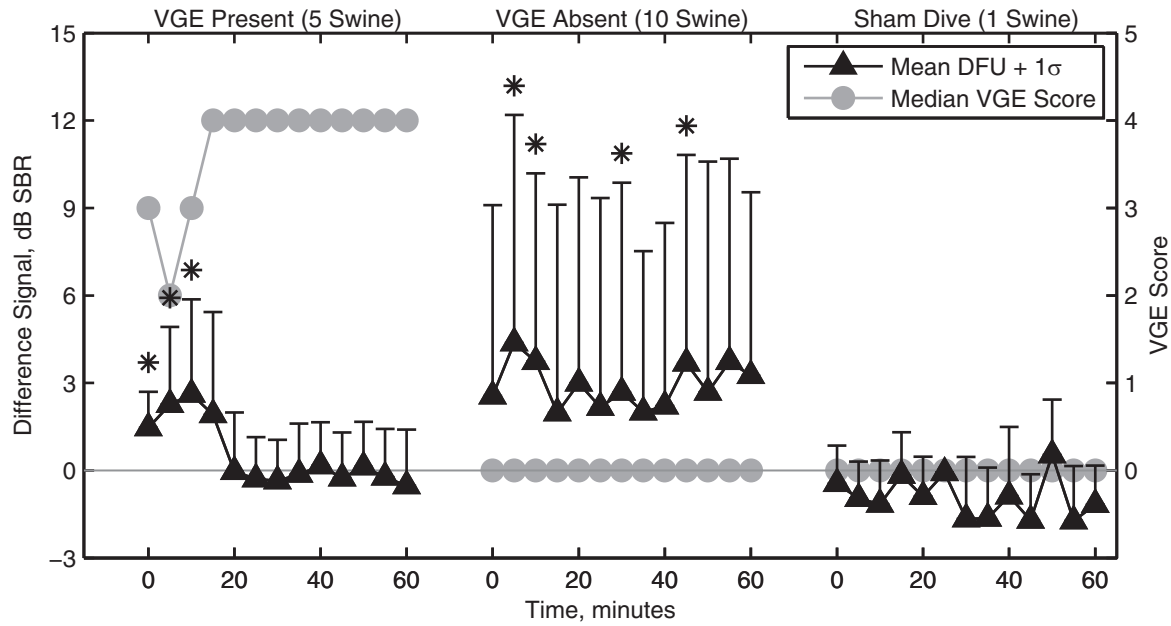

Fig. 5. The VGE and difference signal postdecompression in VGE Present, VGE Absent, and Sham Dive swine. Difference signal was initially elevated above baseline in the VGE Present group, but returned to baseline after 20 min. In VGE Absent swine, difference signal stayed elevated for the entire 60 min measuring period. The Sham swine showed no change in difference signal. $*P < 0.05$ compared with baseline; baseline values not shown on graph for clarity reasons.

crease in the pump and image frequencies. On balance, the results from this study suggest that microbubbles are growing or coalescing to become larger bmdVGE, but further study is needed to establish this unequivocally.

The fact that the bubbles persisted over time without developing into bmdVGE is also an interesting finding. These data suggest that there are microbubbles circulating postdecompression that do not immediately grow into larger bmdVGE. It is not possible to know from the present study whether the detected bubbles are stable microbubbles or whether the population of bubbles is constantly changing, with new microbubbles being formed while other microbubbles are being destroyed or growing outside the detectable diameter range. But, to our knowledge, this is the first demonstration that there may be a population of circulating microbubbles that exist in the bloodstream prior to bmdVGE detection.

Significance. The data from this study strongly suggest that microbubbles precede bmdVGE and can be detected in the absence of bmdVGE. The bmdVGE have been linked to a variety of decompression-associated ailments (9, 12, 14–16, 20), and therefore an early detection method for decompression stress would be of great benefit. For example, if microbubbles appear during an ascent from a dive, the possibility exists that if the diver descended slightly or extended the time at a decompression stop, the microbubbles might disappear and serve as a marker that the ascent could continue safely. Further research would be needed to demonstrate if this is the case.

While the actual implementation of DFU device on a freely moving diver will provide its own set of challenges, the DFU technique itself is well-suited for real-time monitoring. The data from this study show that DFU could be used to monitor at several body sites, which makes this a flexible monitoring technique. The DFU transducers could be placed in locations that do not interfere with the diver's work. Also, DFU is a low-power technique. The industrial transducers and data acquisition and processing equipment used in this study are well-suited for research, but the technique could be implemented using with small, flat transducers and low-power digital signal processors with the power supplied from a battery. Last, the DFU returns a difference signal at a frequency lower than the image frequency, which is likely to be attenuated less in transit.

Limitations. The main objective of this study was to determine if microbubbles could be detected in the bloodstream using DFU. The study was not designed as a head-to-head comparison study with a variety of other ultrasound techniques. So, we cannot rule out that under optimal experimental conditions other B-mode ultrasound and/or Doppler ultrasound devices might have detected a signal in the bloodstream earlier than the instrument we used. This needs to be tested in future studies. But, we believe this is unlikely since the concentration of the microbubbles we detected was most likely much less than the minimum concentration needed to see a bubble on B-mode ultrasound. Also, we compared the devices directly under ideal conditions [the mineral oil tank experiment (Fig. 2)] and showed a significant difference in sensitivity.

Our study used anesthetized swine, not active divers, so more work is needed to show if this technique could be applied to real world human applications. Physically active divers provide data acquisition problems that are more challenging that those found with anesthetized swine. While no research has shown an effect of our anesthetic on VGE production or decompression stress, this does not mean that one does not exist.

The data from this study do not allow for definitive conclusions about the attenuation of the microbubble signal once bmdVGE appeared. Microbubble detection clearly preceded bmdVGE detection in this study, but the reduction in the microbubble signal that was seen once bmdVGE appeared could be due to several factors.

Conclusion. Microbubbles appear in the bloodstream following decompression and can be detected at over both vascular and tissue sites using DFU. The microbubbles occur before bmdVGE and are inversely related to the appearance of bmdVGE. This temporal relationship supports the hypothesis that microbubbles are the precursors for larger bmdVGE. Microbubbles persisted in the absence of bmdVGE. The data also suggest that the DFU technique has potential as a method for early detection of decompression stress.

GRANTS

This work was supported by the Office of Naval Research (ONR N00014-02-1-0406).

DISCLOSURES

No conflicts of interest, financial or otherwise, are declared by the author(s).

AUTHOR CONTRIBUTIONS

Author contributions: J.G.S., J.C.W., and J.C.B. conception and design of research; J.G.S., J.C.W., K.L.M., S.A.K., D.A.K., S.D.P., T.L.B., A.M.F., and J.C.B. performed experiments; J.G.S., J.C.W., and J.C.B. analyzed data; J.G.S., J.C.W., P.J.M., and J.C.B. interpreted results of experiments; J.G.S., J.C.W., and J.C.B. prepared figures; J.G.S., J.C.W., and J.C.B. drafted manuscript; J.G.S., J.C.W., K.L.M., D.A.K., S.D.P., and J.C.B. edited and revised manuscript; J.G.S., J.C.W., and J.C.B. approved final version of manuscript.

REFERENCES

1. **Lantheus Medical Imaging.** Definity: Perfluten Lipid Microsphere, North Billerica, MA: 2013.
2. **Behnke AR.** Physiologic studies pertaining to deep sea diving and aviation, especially in relation to the fat content and composition of the body: The Harvey Lecture, March 19, 1942. *Bull N Y Acad Med* 18: 561–585, 1942.
3. **Blatteau JE, Souraud JB, Gempp E, Boussuges A.** Gas nuclei, their origin, and their role in bubble formation. *Aviat Space Environ Med* 77: 1068–1076, 2006.
4. **Bollinger BR.** Dual-frequency ultrasound detection and sizing of microbubbles for studying decompression sickness: Dissertation. Hanover, NH: Dartmouth College, 2008, p. 194.
5. **Bollinger BR, Wilbur JC, Donoghue TG, Phillips SD, Knaus DA, Magari PJ, Alvarenga DL, Buckey JC.** Dual-frequency ultrasound detection of stationary microbubbles in tissue. *Undersea Hyperb Med* 36: 127–136, 2009.
6. **Brubakk AO, Eftedal O.** Comparison of three different ultrasonic methods for quantification of intravascular gas bubbles. *Undersea Hyperb Med* 28: 131–136, 2001.
7. **Buckey JC, Knaus DA, Alvarenga DL, Kenton MA, Magari PJ.** Dual-frequency ultrasound for detecting and sizing bubbles. *Acta Astronaut* 56: 1041–1047, 2005.
8. **Claudon M, Dietrich CF, Choi BI, Cosgrove DO, Kudo M, Nolsoe CP, Piscaglia F, Wilson SR, Barr RG, Chammas MC, Chaubal NG, Chen MH, Clevert DA, Correas JM, Ding H, Forsberg F, Fowlkes JB, Gibson RN, Goldberg BB, Lassau N, Leen EL, Mattrey RF, Moriyasu F, Solbiati L, Weskott HP, Xu HX, World Federation for Ultrasound in Medicine, and European Federation of Societies for Ultrasound.** Guidelines and good clinical practice recommendations for Contrast Enhanced Ultrasound (CEUS) in the liver - Update 2012: A WFUMB-EFSUMB initiative in cooperation with representatives of AFSUMB, AIUM, ASUM, FLAUS and ICUS. *Ultrasound Med Biol* 39: 187–210, 2013.
9. **Cotes JE.** Respiratory effects of diving. *Eur Respir J* 7: 2–3, 1994.
10. **Dunford RG, Vann RD, Gerth WA, Pieper CF, Huggins K, Wacholtz C, Bennett PB.** The incidence of venous gas emboli in recreational diving. *Undersea Hyperb Med* 29: 247–259, 2002.
11. **Eftedal OS, Lydersen S, Brubakk AO.** The relationship between venous gas bubbles and adverse effects of decompression after air dives. *Undersea Hyperb Med* 34: 99–105, 2007.
12. **Hallenbeck JM, Andersen JC.** Pathogenesis of the decompression disorders. In: *The Physiology and Medicine of Diving*, edited by Bennett PB and Elliott DH. London: Balliere Tindall, 1982, p. 435–460.
13. **Hamilton M, Il'Inskii Y, Zabolotskaya E.** Dispersion. In: *Nonlinear Acoustics*, edited by Hamilton M and Blackstock D. Melville, NY: Acoust Soc of Am, 2008, p. 151–175.
14. **Helps SC, Parsons DW, Reilly PL, Gorman DF.** The effect of gas emboli on rabbit cerebral blood flow. *Stroke* 21: 94–99, 1990.
15. **Hemelryck W, Germonpre P, Papadopoulou V, Rozloznik M, Balestra C.** Long term effects of recreational SCUBA diving on higher cognitive function. *Scand J Med Sci Sports* 2013.
16. **Hills BA, James PB.** Microbubble damage to the blood-brain barrier: Relevance to decompression sickness. *Undersea Biomed Res* 18: 111–116, 1991.
17. **Mahon RT.** Tiny bubbles. *J Appl Physiol* 108: 238–239, 2010.
18. **Minnaert M.** On musical air-bubbles and the sounds of running water. *Philos Mag* 16: 235–248, 1933.
19. **Newhouse VL, Shankar PM.** Bubble size measurements using nonlinear mixing of two frequencies. *J Acoust Soc Am* 75: 1473–1477, 1984.
20. **Skogland S, Segadal K, Sundland H, Hope A.** Gas bubbles in rats after heliox saturation and different decompression steps and rates. *J Appl Physiol* 92: 2633–2639, 2002.
21. **Swan JG, Bollinger BD, Donoghue TG, Wilbur JC, Phillips SD, Alvarenga DL, Knaus DA, Magari PJ, Buckey JC.** Microbubble detection following hyperbaric chamber dives using dual-frequency ultrasound. *J Appl Physiol* 111: 1323–1328, 2011.
22. **Vann RD, Grimstad J, Nielsen CH.** Evidence for gas nuclei in decompressed rats. *Undersea Biomed Res* 7: 107–112, 1980.
23. **Wilbur JC, Phillips SD, Donoghue TG, Alvarenga DL, Knaus DA, Magari PJ, Buckey JC.** Signals consistent with microbubbles detected in legs of normal human subjects after exercise. *J Appl Physiol* 108: 240–244, 2009.
24. **Yount DE.** Growth of bubbles from nuclei. In: *Supersaturation and Bubble Formation in Fluids and Organisms*, edited by Brubakk AO, Hemmingsen BB, and Sundnes G. Trondheim: Tapir, 1988, p. 131–164.